

# Improved Modeling of the Discrete Component of the Galactic Interstellar $\gamma$ -ray Emission and Implications for the *Fermi*–LAT Galactic Center Excess

Christopher M. Karwin,<sup>1,2,\*</sup> Alex Broughton,<sup>2,†</sup> Simona Murgia,<sup>2,‡</sup>  
Alexander Shmakov,<sup>3,§</sup> Mohammadamin Tavakoli,<sup>3,¶</sup> and Pierre Baldi<sup>3,\*\*</sup>

<sup>1</sup>*Department of Physics and Astronomy, Clemson University, Clemson, South Carolina 29634, USA*

<sup>2</sup>*Department of Physics and Astronomy, University of California, Irvine, California 92697, USA*

<sup>3</sup>*Department of Computer Science, University of California, Irvine, California 92697, USA*

(Dated: June 8, 2022)

The aim of this work is to improve models for the  $\gamma$ -ray discrete or small-scale structure related to  $\text{H}_2$  interstellar gas. Reliably identifying this contribution is important to disentangle  $\gamma$ -ray point sources from interstellar gas, and to better characterize extended  $\gamma$ -ray signals. Notably, the *Fermi*–LAT Galactic center (GC) excess, whose origin remains unclear, might be smooth or point-like. If the data contain a point-like contribution that is not adequately modeled, a smooth GC excess might be erroneously deemed to be point-like. We improve models for the  $\text{H}_2$ -related  $\gamma$ -ray discrete emission for a  $50^\circ \times 1^\circ$  region along the Galactic plane via  $\text{H}_2$  proxies better suited to trace these features. We find that these are likely to contribute significantly to the  $\gamma$ -ray *Fermi*–LAT data in this region, and the brightest ones are likely associated with detected *Fermi*–LAT sources, a compelling validation of this methodology. We discuss prospects to extend this methodology to other regions of the sky and implications for the characterization of the GC excess.

The Galactic  $\gamma$ -ray interstellar emission (IE) traces interactions of cosmic rays (CRs) with the interstellar medium, and constitutes most of the  $\gamma$ -ray emission observed by *Fermi*–LAT. Uncertainties in modeling the IE are large and difficult to constrain, and they impact the study of other  $\gamma$ -ray sources in the *Fermi*–LAT data, point-like as well as extended. We focus on modeling the small-scale structure of the IE which, if not robustly captured by the model, confuses the determination of point sources, especially along the Galactic plane [1]. It was shown in [2] that a large fraction of the point sources detected by *Fermi*–LAT in the Galactic Center (GC) region could be misidentified gas structure, and strongly dependent in number and spatial distribution on the IE model employed to analyze the data. This result indicates the presence of point-like emission in the data arising from unmodeled structure in the interstellar gas, and it underlines the importance of accurately modeling this component to reliably identify point sources in the  $\gamma$ -ray data.

More reliable modeling of the small scale gas structure could also impact the characterization of extended sources. A prominent example is the *Fermi*–LAT GC excess [2–8]. Striking features of this excess are its spatial morphology and spectrum which are compatible with annihilating dark matter (DM). Alternative explanations have been proposed, with the leading one attributing the signal to a collection of discrete emitters such as an unresolved point source population of millisecond pul-

sars. The origin of the *Fermi*–LAT GC excess remains a debated topic [9]. This debate could be settled by determining whether the spatial morphology of the excess is consistent with a smooth distribution, as predicted for DM, or with the cumulative emission of a collection of point-like emitters. Statistical techniques have been employed to accomplish this [10–13], including the non-Poissonian template fit (NPTF) which can detect upward fluctuations in the photon statistics above Poisson noise which are associated with a collection of point sources. However, the results of the NPTF technique strongly depend on the modeling of the IE, and an uncontroversial resolution to the origin of the GC excess has not yet been reached. We posit that if the interstellar gas is more structured and point-like than current models predict, the unresolved point source contribution in the data could be erroneously inflated by the fainter component (also below detection threshold) of the small scale gas features. In particular, statistical methods such as the NPTF might attribute this component to a smooth GC excess and conclude it is point-like. These uncertainties might therefore hinder the ability to distinguish the smooth versus point-like duplicity of the excess. We note that wavelet decomposition is another statistical technique that has been employed to resolve the GC excess. While these studies are not as impacted by the IE model, the related results on the nature of the GC excess remain uncertain nonetheless [10, 14, 15].

In this work, we present a novel approach to improve modeling of the small-scale structure in the interstellar gas. The IE is due primarily to CRs interacting with the interstellar hydrogen gas (and radiation field), in molecular ( $\text{H}_2$ ), atomic (HI), and ionized (HII) forms.  $\text{H}_2$  and HI are highly structured compared to HII, and this structure is traced by the related  $\gamma$ -ray emission. In this work, we focus on  $\text{H}_2$  gas because of its high degree of structure and our methodology hinges on the availability of additional proxies better suited to model it. The impact of the other components of the  $\gamma$ -ray IE (specifically HI and dark gas [16]), and related uncertainties, is not considered in this study and will be the focus of later work. Since  $\text{H}_2$  does not emit at a characteristic radio frequency, other molecules are used to trace its distribution. In particular, carbon monoxide ( $^{12}\text{CO}$ , or CO hereafter) is typically employed as a proxy. Radio surveys trace the distribution of CO across the sky and the  $\text{H}_2$  column density is inferred by scaling the CO content by a conversion factor ( $X_{\text{CO}}$ ) which gives the ratio of the integrated CO line emission to the  $\text{H}_2$  column density. The bulk of the  $\text{H}_2$  is traced following this methodology, and the survey of the CO  $J=1-0$  transition line from [17] has been widely employed. However, CO is typically optically thick in the denser cores of molecular clouds and it underestimates the total  $\text{H}_2$  column density there.  $\gamma$ -ray IE models that employ CO to trace  $\text{H}_2$  gas may therefore underestimate its finer structure. This limitation can be addressed by exploiting CO isotopologues,  $^{13}\text{CO}$  and  $\text{C}^{18}\text{O}$ , also found in  $\text{H}_2$  clouds. Although rarer, these isotopologues are not as optically thick and therefore more reliable to probe dense cores.

We employ the data from the Mopra Southern Galactic Plane CO Survey (data release 3) [18] to trace the denser  $\text{H}_2$  regions. The survey covers a 50 square degree region, spanning Galactic longitudes  $l = 300^\circ$ - $350^\circ$  and latitudes  $|b| \leq 0.5^\circ$ , and it targets the  $J = 1-0$  transitions of CO,  $^{13}\text{CO}$ ,  $\text{C}^{18}\text{O}$ , and  $\text{C}^{17}\text{O}$ . The data reduction process, which involves six main stages of processing to perform the band-pass correction and background subtraction, yields data cubes of the brightness temperature for each spectral line, as a function of Galactic coordinates and local standard of rest velocity. Mopra’s observations are carried out in  $1^\circ \times 1^\circ$  segments, which we combine into a mosaic for the full region. To ensure the highest quality data in the rare isotopologues, only pixels for which the brightness temperature exceeds the  $1\sigma$  noise provided by Mopra are used. This step is necessary since the noise could otherwise predict spurious  $\gamma$ -ray emission. In this analysis we utilize the CO and  $^{13}\text{CO}$  data,

as the  $\text{C}^{18}\text{O}$  emission is extremely sparse, and the  $\text{C}^{17}\text{O}$  emission was too faint to be detected in the survey. The spatial resolution is  $0.6'$  and the spectral resolution is  $0.1 \text{ km sec}^{-1}$ . For the region it surveys, the Mopra data provide a sharper view of the CO emission compared to [17], in addition to probing the rarer  $\text{H}_2$  tracers.

We calculate the  $\text{H}_2$  column density corresponding to Mopra’s CO and  $^{13}\text{CO}$ , referred to as  $N(\text{H}_2)_{\text{CO}}$  and  $N(\text{H}_2)_{\text{CO}13}$ , respectively. Following the method of [19], the gas is separated into 17 Galactocentric radial bins based on its velocity and therefore corresponding to different distances from the GC, assuming uniform circular motion about the GC. The  $N(\text{H}_2)_{\text{CO}}$  is determined as:

$$N(\text{H}_2)_{\text{CO}} = W(\text{CO}) \times X_{\text{CO}}, \quad (1)$$

where  $W(\text{CO})$  is the line strength of the CO gas, and we adopt the radially-dependent  $X_{\text{CO}}$  from [19] for the 17 radial bins.

$N(\text{H}_2)_{\text{CO}13}$  is evaluated as:

$$N(\text{H}_2)_{\text{CO}13} = N(\text{CO}13) \times \left[ \frac{\text{H}_2}{\text{CO}13} \right]. \quad (2)$$

Following [18, 20], we derive the  $^{13}\text{CO}$  column density  $N(\text{CO}13)$  assuming that the gas is in local thermodynamic equilibrium at a fixed excitation temperature of 10 K. For the abundance ratio  $\left[ \frac{\text{H}_2}{\text{CO}13} \right]$ , we choose the upper bound of the range  $(2.7 - 7.5) \times 10^5$  provided in [21], in an attempt to assess the maximal impact on the  $\gamma$ -ray data, although it is not excluded that larger values are possible.

The CR propagation code GALPROP (v56) [22–32] is used to evaluate the  $\gamma$ -ray intensity maps for the  $\text{H}_2$ -related emission traced by CO and  $^{13}\text{CO}$ . GALPROP self-consistently calculates spectra and abundances of Galactic CR species and associated diffuse emissions ( $\gamma$ -rays, but also radio, X-rays) in 2D and 3D. We adopt the same GALPROP input parameters as described in [33]. GALPROP returns radially dependent  $\gamma$ -ray intensity all-sky maps (in 17 Galactocentric annuli) which allow us to determine, for the region observed by Mopra, the additional contribution in  $\gamma$ -rays from the  $\text{H}_2$  traced by  $^{13}\text{CO}$ , and assess its significance in simulated *Fermi*-LAT data. The difference between  $N(\text{H}_2)_{\text{CO}13}$  and  $N(\text{H}_2)_{\text{CO}}$  gives an estimate of the  $\text{H}_2$  that is missed in dense regions when only CO is used as a tracer. To calculate the corresponding intensity in  $\gamma$ -rays, we define the “Modified Map”. This is calculated in the following way: for pixels with  $N(\text{H}_2)_{\text{CO}13} > N(\text{H}_2)_{\text{CO}12}$ , the value of  $N(\text{H}_2)_{\text{CO}12}$  is replaced with the value of  $N(\text{H}_2)_{\text{CO}13}$ . We define the

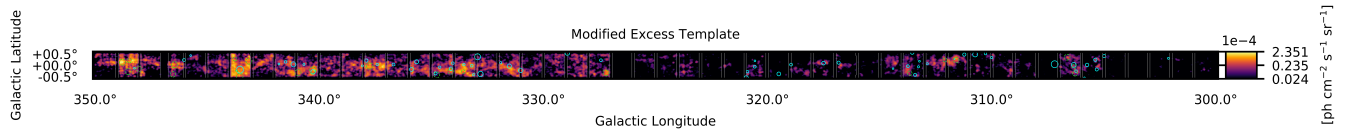


FIG. 1. The Modified Excess Template, calculated as the difference between the Modified Map and the baseline CO map. The color scale shows the  $\gamma$ -ray intensity. The solid cyan circles show unassociated  $\gamma$ -ray point sources in version 4FGL-DR2 of the fourth *Fermi*-LAT catalog [34], and the dashed green circles show new sources, not in the 4FGL-DR2, that we find in this work (see text). The radius of each source corresponds to the 95% localization uncertainty.

“Modified Excess Template” as the difference between the Modified Map and the baseline CO map, which accounts for the additional  $\text{H}_2$ -related  $\gamma$ -ray emission not included in current IE models, shown in Fig. 1.

We evaluate the significance of the Modified Excess Template in the *Fermi*-LAT data by simulating the data collected between 2008 August 04 to 2020 November 11 ( $\sim 12$  years). The simulated events have energies in the range 1 – 100 GeV and are binned in 8 energy bins per decade, for event class P8R3-CLEAN (FRONT+BACK). The analysis is performed using Fermipy (v0.19.0), which utilizes the Fermitools (v1.2.23). In these simulations, we only focus on the  $\text{H}_2$ -related  $\gamma$ -ray emission, and exclude all other components of the  $\gamma$ -ray sky. The goal is to assess the significance of the Modified Excess Template, i.e. the contribution of the newly modeled  $\text{H}_2$  fine structure, in the optimistic scenario where all other components are satisfactorily modeled. The simulated events trace the  $\text{H}_2$ -related  $\gamma$ -ray emission modeled with the Modified Map. The simulated data are then fit based on a binned maximum likelihood method to a model that includes two components, the  $\gamma$ -rays traced by the baseline CO map and the Modified Excess Template. The latter is assigned the spectrum determined by GALPROP, and its normalization is free to vary in the fit. The normalization of the CO map is also free to vary and its spectrum constrained to that calculated by GALPROP. As mentioned above, the  $\gamma$ -ray flux is calculated in 17 radial bins, since the predicted  $\text{H}_2$ -related  $\gamma$ -ray emission depends on the CR density, which is a function of Galactocentric radius. In the simulations, the total emission is integrated along the line-of-sight. Moreover, the individual maps have a high level of degeneracy. We therefore combine the maps into 4 radial bins. Specifically, we combine bins 1-6, 7-10, 11-13, and 14-17, which we refer to as A1, A2, A3, and A4.

We simulate 1000 realizations of *Fermi*-LAT data, and calculate the Test Statistics (TS) for the nested models ( $-2\log(L_0/L)$ ), where  $L_0$  corresponds to value of the likeli-

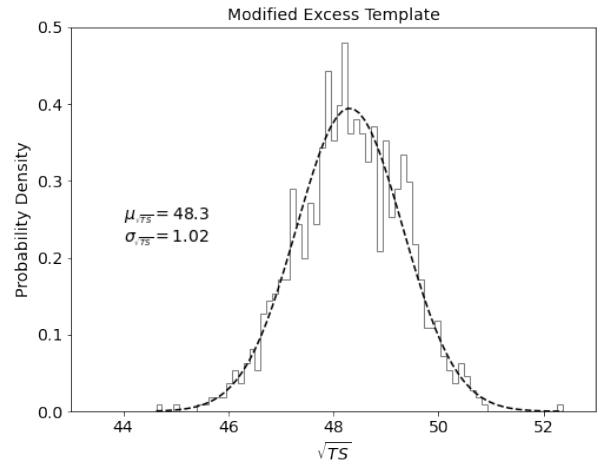


FIG. 2. Distribution of the statistical significance ( $\sigma \approx \sqrt{\text{TS}}$ ) of the Modified Excess Template for the  $50^\circ \times 1^\circ$  region covered by Mopra for 1000 realizations of  $\sim 12$  years of *Fermi*-LAT data. A fit with a Gaussian function is overlaid.

hood function for the null hypothesis (CO baseline), and L to the alternative hypothesis (CO baseline and Modified Excess Template.) The statistical significance is approximated by  $\sigma \approx \sqrt{\text{TS}}$ . The distribution of the  $\sqrt{\text{TS}}$  for the 1000 simulations is shown in Fig. 2. The mean of the distribution is  $48.30 \pm 1.02$ , for the 50 squared degree Mopra region, and therefore very significant in a scenario where other components contributing to the *Fermi*-LAT data are perfectly modeled, and if the  $\gamma$ -ray emission traced by  $^{13}\text{CO}$  is at the high end of the range we have considered (with the caveats discussed above.)

The fractional residuals as a function of energy for the 1000 simulations are shown in Fig. 3. They are consistent with zero, as expected. Fig. 4 shows the distributions of the flux of each model component, including the Modified Excess Template. In the Mopra region, the mean integrated flux is  $(7.2 \pm 0.2) \times 10^{-8} \text{ ph cm}^{-2} \text{ s}^{-1}$ . Overall, the Modified Excess Template accounts for a fair fraction (15.4%) of the total  $\text{H}_2$ -related  $\gamma$ -ray emis-

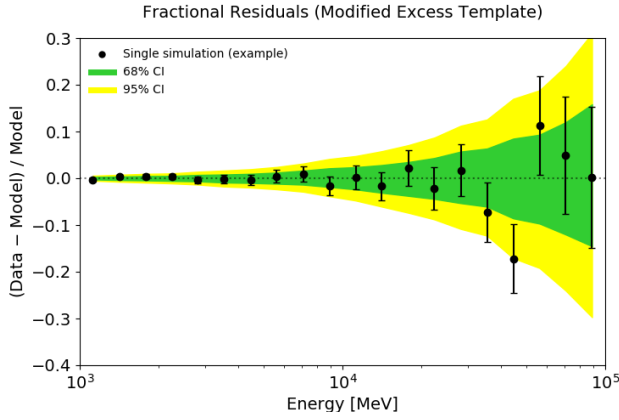


FIG. 3. Fractional count residuals as a function of energy. The green and yellow bands show the 68% and 95% confidence regions from 1000 simulations, respectively. As an example, we also plot the results for a single simulation, shown with black data points.

sion in the Mopra region. For comparison, the integrated GC excess flux in a  $15^\circ \times 15^\circ$  region around the GC, which is  $4\times$  larger than the region observed by Mopra, is in the range  $18.3 - 25.0 \times 10^{-8} \text{ ph cm}^{-2} \text{ s}^{-1}$  (from [2]). In intensities, the GC excess corresponds to  $2.67 - 3.65 \times 10^{-6} \text{ ph cm}^{-2} \text{ s}^{-1} \text{ sr}^{-1}$  compared to  $4.72 \times 10^{-6} \text{ ph cm}^{-2} \text{ s}^{-1} \text{ sr}^{-1}$  for the Modified Excess Template. Because of the different spatial morphology of the GC excess and  $\text{H}_2$ -related  $\gamma$ -ray emission traced by  $^{13}\text{CO}$ , a direct comparison is unwarranted and we do not expect the latter to account for the majority of the GC excess. However, the  $\text{H}_2$  emission extends beyond the latitudes considered in this study and, albeit dimmer at higher latitudes, the estimates provided here do not indicate its small scale component to be negligible. This contribution could therefore confuse the GC excess morphology, depending on the exact  $\text{H}_2$  emission outside of  $\pm 0.5^\circ$  in latitude, because the techniques that track the point-like fluctuations could erroneously ascribe unaccounted point-like emission (originating from  $\text{H}_2$  gas in this case) to the GC excess [12]. Considerations based on the spectrum of the unresolved source population could be powerful to settle this degeneracy, however a robust determination is required.

We identify the structure traced by  $^{13}\text{CO}$  that is bright enough to be detected as a *Fermi*-LAT point source and compare it to the unassociated sources in version 4FGL-DR2 of the fourth *Fermi*-LAT catalog of  $\gamma$ -ray sources [34]. A significant overlap would indicate that its brightest contribution has already been detected by *Fermi*-LAT and validate the methodology to trace this

component. To this end, we perform a likelihood fit where, instead of including the Modified Excess Template in the model, we only consider the baseline CO map and find additional point sources using the *fermipy find\_srcs* function. The method calculates TS maps, and identifies point sources based on peaks in the TS. We use a test point source modeled with a power law spectrum with spectral index=2, and a minimum TS threshold of  $\text{TS} \geq 16$ . An index of 2.7 is compatible with CRs interacting with gas, and if used, it yields consistent results. In total we find 23 new point sources with  $\text{TS} \geq 16$ , which are shown with green circles in Fig. 1. For comparison, we also overlay 4FGL-DR2 unassociated sources. We find that 8/23 (35%) of the new sources are spatially consistent with an unassociated 4FGL-DR2 source (based on an overlap of the 95% localization errors), which accounts for 8/46 (17%) of the total unassociated sources in the region. To quantify the probability that the associations happen by chance, we perform 1000 simulations, where for each realization we randomly distribute 23 sources in the Mopra region. For each source the Galactic coordinates are drawn from a uniform distribution and we assign an error radius drawn from a Gaussian distribution, with the mean and standard deviation determined from the 23 detected sources. From the 1000 simulations we find the average number of random associations to be  $3.16 \pm 1.72$ , which corresponds to a p-value (i.e.  $N(\geq 8)/1000$ ) of 0.012. It is therefore likely that the brightest of the point-like emission traced by Mopra  $^{13}\text{CO}$  have already been detected in the *Fermi*-LAT data.

The results presented here demonstrate that there likely is significant structure in the  $\text{H}_2$ -related  $\gamma$ -ray emission detected by *Fermi*-LAT that is not currently included in the IE models. Since its spatial morphology has point-like features, it directly affects the detection of resolved and, potentially, unresolved point source populations in the  $\gamma$ -ray data. More specifically, we have discussed the impact on the 4FGL-DR2 catalog and on the interpretation of the GC excess. Although in this analysis we have focused on the region covered by Mopra, similar conclusions would hold elsewhere because of the same limitations in tracing  $\text{H}_2$ . The methodology described here however can only be readily applied to very small regions of the sky because of the paucity of observations of the rare  $\text{H}_2$  tracers (e.g. [35]). Also, we cannot simply extrapolate the Modified Excess Template with the less ambitious goal of providing only an estimate of this emission since the Mopra data on which it is based is tightly confined, especially in latitude. To address the limited available observations, we have resorted to ma-

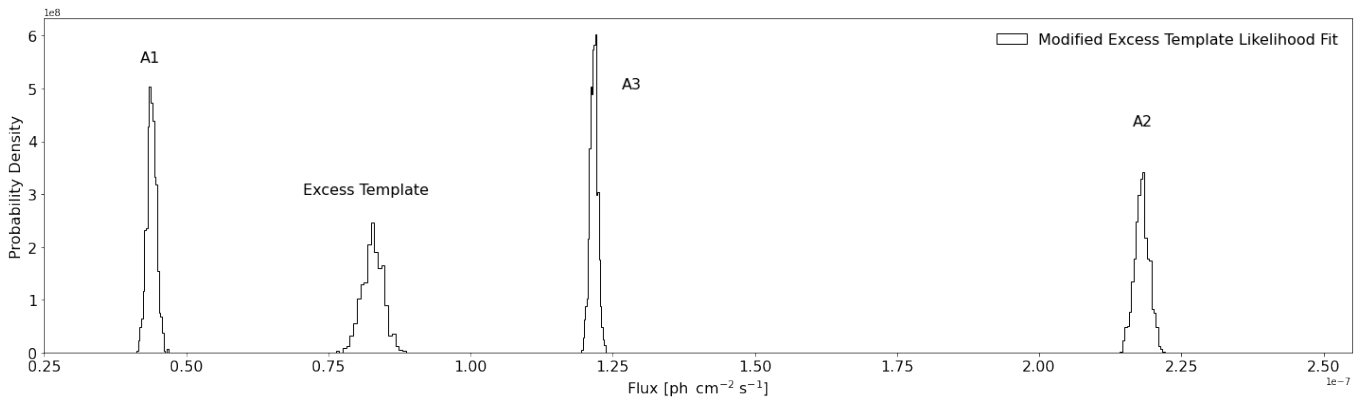


FIG. 4. The distributions of fluxes for each component of the best-fit model using the Modified Excess Template over the full region for 1000 realizations of  $\sim 12$  years of *Fermi*-LAT data. Note that one of the annuli (A4) has negligible contribution and the normalization was fixed in the fitting process (corresponding to a flux of  $4.98 \times 10^{-9}$   $\text{ph cm}^{-2} \text{s}^{-1}$ ).

chine learning to develop a methodology that predicts the distribution of the small scale  $\text{H}_2$ -related  $\gamma$ -ray emission for other regions of the sky based on the existing Mopra data. Because of its complexity, we describe the machine related work in a companion paper [36].

*Conclusions.*— We assess whether there is point-like emission in the  $\gamma$ -ray data associated with the interstellar gas and not currently included in models of the Galactic interstellar  $\gamma$ -ray emission. We employ the data from the Mopra Southern Galactic Plane CO Survey, which includes tracers of the small scale structure of the  $\text{H}_2$ -related  $\gamma$ -rays, to improve models by more accurately describing the point-like features in the gas. We find that significant point-like emission originates from  $\text{H}_2$  gas and the significance could be as high as  $\sqrt{TS} \sim 48$  (depending on assumptions) in a  $50^\circ \times 1^\circ$  region covered by Mopra, corresponding to  $\sim 15\%$  of the modeled  $\text{H}_2$ -related  $\gamma$ -ray emission in the region. We also show that this newly found point-like component may account for some fraction ( $\lesssim 17\%$ ) of  $\gamma$ -ray point sources detected by *Fermi*-LAT in the Galactic plane whose origin is so far unknown. That a significant number of unidentified 4FGL-DR2 sources along the Galactic plane originate from unmodelled structure in the gas is not unexpected, but here we develop a robust and reliable methodology to identify the contribution of both bright and dimmer components of the  $\text{H}_2$  gas discrete emission. Given the significance of this emission, its contribution in the GC region could introduce a significant systematic uncertainty in determining whether the GC excess is smooth or point-like, and therefore more consistent with a dark matter or pulsar interpretation, specifically when relying on statistical techniques such as the NPTF. Identifying this component in the GC region could be a crucial step to settle the ori-

gin of the GC excess and to reliably determine whether it is smooth and therefore a signal from DM.

## ACKNOWLEDGEMENTS

We thank Troy Porter for many helpful discussions and insights. The work of AS, MT, and PB is in part supported by grants NSF NRT 1633631 and ARO 76649-CS to PB.

---

\* ckarwin@clemson.edu

† abrought@uci.edu

‡ smurgia@uci.edu

§ ashmakov@uci.edu

¶ mohamadt@uci.edu

\*\* pfbaldi@uci.edu

- [1] S. Abdollahi *et al*, Fermi large area telescope fourth source catalog, The Astrophysical Journal Supplement Series **247**, 33 (2020).
- [2] M. Ajello, A. Albert, W. Atwood, G. Barbiellini, D. Bastieri, K. Bechtol, R. Bellazzini, E. Bissaldi, R. Blandford, E. Bloom, *et al.*, Fermi-lat observations of high-energy  $\gamma$ -ray emission toward the galactic center, The Astrophysical Journal **819**, 44 (2016).
- [3] L. Goodenough and D. Hooper, Possible evidence for dark matter annihilation in the inner milky way from the fermi gamma ray space telescope (2009), arXiv:0910.2998 [hep-ph].
- [4] D. Hooper and L. Goodenough, Dark Matter Annihilation in The Galactic Center As Seen by the Fermi Gamma Ray Space Telescope, Phys. Lett. B **697**, 412 (2011), arXiv:1010.2752 [hep-ph].
- [5] K. N. Abazajian, The consistency of fermi-LAT observations of the galactic center with a millisecond pulsar

- population in the central stellar cluster, *Journal of Cosmology and Astroparticle Physics* **2011** (03), 010.
- [6] K. Abazajian, N. Canac, S. Horiuchi, and M. Kaplinghat, Astrophysical and dark matter interpretations of extended gamma ray emission from the galactic center, *Physical Review D* **90** (2014).
- [7] F. Calore, I. Cholis, and C. Weniger, Background model systematics for the fermi GeV excess, *Journal of Cosmology and Astroparticle Physics* **2015** (03), 038.
- [8] T. Daylan, D. P. Finkbeiner, D. Hooper, T. Linden, S. K. Portillo, N. L. Rodd, and T. R. Slatyer, The characterization of the gamma-ray signal from the central milky way: A case for annihilating dark matter, *Physics of the Dark Universe* **12**, 1 (2016).
- [9] S. Murgia, The fermi-lat galactic center excess: Evidence of annihilating dark matter?, *Annual Review of Nuclear and Particle Science* **70**, 455 (2020), <https://doi.org/10.1146/annurev-nucl-101916-123029>.
- [10] R. Bartels, S. Krishnamurthy, and C. Weniger, Strong support for the millisecond pulsar origin of the Galactic center GeV excess, *Phys. Rev. Lett.* **116**, 051102 (2016), arXiv:1506.05104 [astro-ph.HE].
- [11] S. K. Lee, M. Lisanti, B. R. Safdi, T. R. Slatyer, and W. Xue, Evidence for unresolved  $\gamma$ -ray point sources in the inner galaxy, *Phys. Rev. Lett.* **116**, 051103 (2016).
- [12] R. K. Leane and T. R. Slatyer, Revival of the Dark Matter Hypothesis for the Galactic Center Gamma-Ray Excess, *Phys. Rev. Lett.* **123**, 241101 (2019), arXiv:1904.08430 [astro-ph.HE].
- [13] Y.-M. Zhong, S. D. McDermott, I. Cholis, and P. J. Fox, Testing the Sensitivity of the Galactic Center Excess to the Point Source Mask, *Phys. Rev. Lett.* **124**, 231103 (2020), arXiv:1911.12369 [astro-ph.HE].
- [14] B. Balaji, I. Cholis, P. J. Fox, and S. D. McDermott, Analyzing the gamma-ray sky with wavelets, *Phys. Rev. D* **98**, 043009 (2018), arXiv:1803.01952 [astro-ph.HE].
- [15] Y.-M. Zhong, S. D. McDermott, I. Cholis, and P. J. Fox, Testing the Sensitivity of the Galactic Center Excess to the Point Source Mask, *Phys. Rev. Lett.* **124**, 231103 (2020), arXiv:1911.12369 [astro-ph.HE].
- [16] I. A. Grenier, J.-M. Casandjian, and R. Terrier, Unveiling Extensive Clouds of Dark Gas in the Solar Neighborhood, *Science* **307**, 1292 (2005).
- [17] T. M. Dame, D. Hartmann, and P. Thaddeus, The Milky Way in Molecular Clouds: A New Complete CO Survey, *Astrophys. J.* **547**, 792 (2001), arXiv:astro-ph/0009217 [astro-ph].
- [18] C. Braiding, G. F. Wong, N. I. Maxted, D. Romano, M. G. Burton, R. Blackwell, M. D. Filipović, M. S. R. Freeman, B. Indermuhle, and J. Lau, *et al.*, The mpra southern galactic plane co survey—data release 3, *Publications of the Astronomical Society of Australia* **35**, 10.1017/pasa.2018.18 (2018).
- [19] M. Ackermann, M. Ajello, W. Atwood, L. Baldini, J. Ballet, G. Barbiellini, D. Bastieri, K. Bechtol, R. Bellazzini, B. Berenji, *et al.*, Fermi-lat observations of the diffuse  $\gamma$ -ray emission: implications for cosmic rays and the interstellar medium, *The Astrophysical Journal* **750**, 3 (2012).
- [20] T. L. Wilson, K. Rohlfs, and S. Hüttemeister, *Tools of Radio Astronomy* (2009).
- [21] J. E. Pineda, P. Caselli, and A. A. Goodman, CO Isotopologues in the Perseus Molecular Cloud Complex: the X-factor and Regional Variations, *Astrophys. J.* **679**, 481 (2008), arXiv:0802.0708 [astro-ph].
- [22] I. V. Moskalenko and A. W. Strong, Production and propagation of cosmic ray positrons and electrons, *Astrophys. J.* **493**, 694 (1998), arXiv:astro-ph/9710124 [astro-ph].
- [23] I. V. Moskalenko and A. W. Strong, Anisotropic inverse compton scattering in the galaxy, *Astrophys. J.* **528**, 357 (2000), arXiv:astro-ph/9811284 [astro-ph].
- [24] A. W. Strong and I. V. Moskalenko, Propagation of cosmic-ray nucleons in the galaxy, *Astrophys. J.* **509**, 212 (1998), arXiv:astro-ph/9807150 [astro-ph].
- [25] A. W. Strong, I. V. Moskalenko, and O. Reimer, Diffuse continuum gamma-rays from the galaxy, *Astrophys. J.* **537**, 763 (2000), [Erratum: *ApJ* 541,1109(2000)], arXiv:astro-ph/9811296 [astro-ph].
- [26] V. S. Ptuskin, I. V. Moskalenko, F. C. Jones, A. W. Strong, and V. N. Zirakashvili, Dissipation of Magneto-hydrodynamic Waves on Energetic Particles: Impact on Interstellar Turbulence and Cosmic-Ray Transport, *Astrophys. J.* **642**, 902 (2006), astro-ph/0510335.
- [27] A. W. Strong, I. V. Moskalenko, and V. S. Ptuskin, Cosmic-ray propagation and interactions in the Galaxy, *ARNPS* **57**, 285 (2007), arXiv:astro-ph/0701517 [astro-ph].
- [28] A. E. Vladimirov, S. W. Digel, G. Johannesson, P. F. Michelson, I. V. Moskalenko, P. L. Nolan, E. Orlando, T. A. Porter, and A. W. Strong, GALPROP WebRun: an internet-based service for calculating galactic cosmic ray propagation and associated photon emissions, *Comput. Phys. Commun.* **182**, 1156 (2011), arXiv:1008.3642 [astro-ph.HE].
- [29] G. Jóhannesson *et al.*, Bayesian analysis of cosmic-ray propagation: evidence against homogeneous diffusion, *Astrophys. J.* **824**, 16 (2016), arXiv:1602.02243 [astro-ph.HE].
- [30] T. A. Porter, G. Johannesson, and I. V. Moskalenko, High-energy gamma rays from the milky way: Three-dimensional spatial models for the cosmic-ray and radiation field densities in the interstellar medium, *Astrophys. J.* **846**, 23pp (2017).
- [31] G. Johannesson, T. A. Porter, and I. V. Moskalenko, The Three-Dimensional Spatial Distribution of Interstellar Gas in the Milky Way: Implications for Cosmic Rays and High-Energy Gamma-Ray Emissions, *Astrophys. J.* **856**, 45 (2018), arXiv:1802.08646 [astro-ph.HE].
- [32] Y. Génolini, D. Maurin, I. V. Moskalenko, and M. Unger, Current status and desired precision of the isotopic production cross sections relevant to astrophysics of cosmic rays: Li, be, b, c, and n, *PhRvC* **98**, 034611 (2018).
- [33] C. M. Karwin, S. Murgia, S. Campbell, and I. V. Moskalenko, Fermi-lat observations of  $\gamma$ -ray emission toward the outer halo of m31, *The Astrophysical Journal* **880**, 95 (2019).

- [34] J. Ballet, T. H. Burnett, S. W. Digel, and B. Lott, Fermi Large Area Telescope Fourth Source Catalog Data Release 2, arXiv e-prints , arXiv:2005.11208 (2020), arXiv:2005.11208.
- [35] R. Blackwell, M. Burton, and G. Rowell, Mopra central molecular zone carbon monoxide survey status, Proceedings of the International Astronomical Union **11**, 164–165 (2016).
- [36] A. Shmakov, M. Tavakoli, P. Baldi, C. Karwin, A. Broughton, and S. Murgia, Deep learning models of the discrete component of the galactic interstellar  $\gamma$ -ray emission (2022).